

# Energy management using predictive control and Neural Networks in microgrid with hybrid storage system

Carlos Fustero, Alejandro Clemente, Ramon Costa-Castelló, Carlos Ocampo-Martinez  
*Institut de Robòtica i Informàtica Industrial*  
*Universitat Politècnica de Catalunya*  
Barcelona, Spain

**Abstract**—Energy storage systems can provide a solution for the current challenges derived from the increasing penetration of renewable energies. Each energy storage system has different characteristics so their combination can be the best solution to achieve the requirements of a given scenario. To achieve the maximum potential of the Energy storage system they must be supplied with an optimal control strategy. Traditional control strategies only focus on increasing self consumption and do not take into consideration future generation and load. Model predictive control can use load and generation forecasts to provide a multi-objective solution which takes into consideration energy storage system degradation, grid congestion and self consumption between others. Neural networks are used to obtain the generation and load forecast, trained with empirical data from real households. An online model based predictive controller implemented for a grid composed by one lithium-ion battery, one vanadium redox flow battery, photovoltaic generation and electric consumption of 14 households. Finally the results of the classical method of maximizing self consumption, the ideal predictive controller considering perfect forecast and the real predictive controller are shown and discussed.

**Index Terms**—Energy management, hybrid energy storage systems, Model predictive control, Neural Networks

## I. INTRODUCTION

The increasing importance of renewable energy sources (RES) and their integration with the electric grids have brought many new challenges concerning voltage regulation, stability and power quality in the grids [1]. For further use of RES in electrical grids, the problems due to their non-dispatch-able and intermittent nature should be addressed.

The use of photovoltaic panel (PV) systems combined with energy storage systems (ESS) has been proved useful to mitigate these issues [2] [3]. Different ESS have different power and energy capabilities so combined they offer more potential in electrical systems [4]. ESS with high-energy storage capabilities, such as Fuel cells (FC)-electrolyser systems [5], [6] and redox flow batteries (RFB) [7], have generally

This research is part of the CSIC program for the Spanish Recovery, Transformation and Resilience Plan funded by the Recovery and Resilience Facility of the European Union, established by the Regulation (EU) 2020/2094, CSIC Interdisciplinary Thematic Platform (PTI+) Transición Energética Sostenible+ (PTI-TRANSENER+ project TRE2103000), the Spanish Ministry of Science and Innovation under projects MAFALDA (PID2021-126001OB-C31 funded by MCIN/AEI/ 10.13039/501100011033 / ERDF/EU), and MASHED (TED2021-129927B-I00), and by the Spanish Ministry of Universities funded by the European Union - NextGenerationEU (2022UPC-MS-93823)

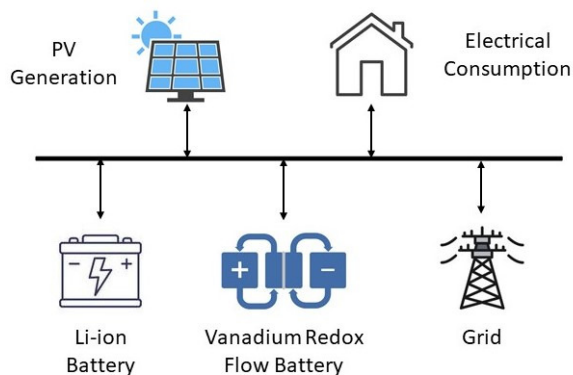


Fig. 1. Microgrid scheme.

a slow dynamic response and lower efficiencies. In contrast, ESS with high power capabilities, such as supercapacitors or flywheels, have an excellent dynamic response but can store a small amount of energy. In the middle of the spectrum would lay ESSs such as Li-ion or conventional batteries. According to the given scenario, the optimal combination and dimension of each ESS should be found.

To obtain the maximum performance, a proper energy management control should be established. The energy management strategy should take into consideration multiple objectives such as reducing battery degradation, avoiding grid congestion and maximizing self consumption (MSC). However, most of the conventional strategies focus only on the latter.

Only focusing in self consumption can lead to grid saturation. The MSC strategy charges all the extra generation into the ESS leading to early charge in high generation days (Fig. 2). Then, when the generation peak is reached, the ESS cannot store more energy and it has to be completely absorbed by the grid, which could saturate it [1].

Another main aspect to take into account is ESS degradation. Though analysing battery degradation is a complicated issue, high charging or discharging powers or maintaining a high state of charge (SOC) are factors that increase degradation in Li-ion batteries [8] [9]. The MSC strategy tries to

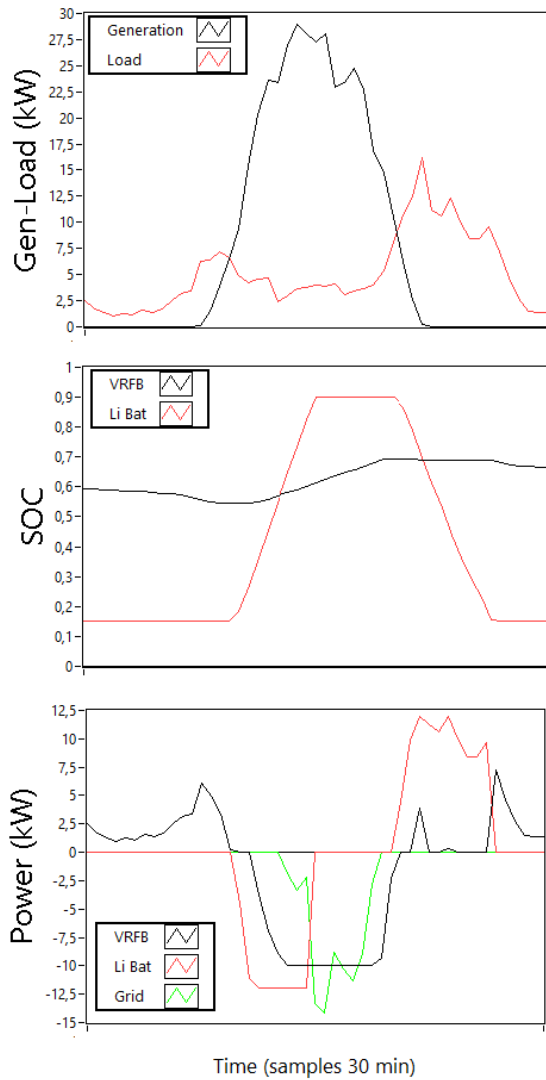


Fig. 2. MSC under high generation in PV, Li-ion and RFB system.

use the ESS as much as possible to compensate generation an load differences leading to high charge and discharge powers. By taking into consideration future loads or generation, the battery could be either charged or discharged slower, reducing its degradation. Additionally, if the battery remains at high SOC's, its degradation is increased.

Model predictive control (MPC) is a control strategy that uses a model of the system to predict its future evolution [10]. As future states can be obtained using the model, the optimal control action can be found by minimizing a cost function. By defining properly such a function, several goals like grid congestion, ESS degradation and self consumption can be simultaneously taken into account. MPC can include future inputs forecast and would be able to be implemented online [11]. Although the MSC strategy could be modified to include forecast information, due to rule-based nature, it is difficult to guarantee that it provides an optimal solution.

To simulate the generation and consumption of the grid, data from a collection of households with PV generation in

Australia has been used [12]. A generation and load predictor of the grid will be implemented in order to supply the MPC with a generation and consumption forecasts. The forecast will be obtained using Neural networks (NN), a machine learning method which obtains information from previous empirical data to make future predictions. Their use has extended significantly in the last decade and previous works show promising results in PV generation and load demand forecasts [13] [14].

The remainder of the paper has the following structure: Section II describes the microgrid justifying the component selection. Section III explains the forecast units fundamentals, structures and the input data available. Section IV explains the MPC fundamentals, cost function, system model and constrains. Section V presents the main results and finally conclusions are summarized in Section VI.

## II. SYSTEM DESCRIPTION

This work implements an MPC controller in a PV hybrid ESS system consisting in a RFB and a lithium-ion battery connected to the grid (Fig. 1). The potential of the RFB lays on the fact that they can increase their energy capacity just by increasing the tank size of its electrolytes. Additionally, as the electrolytes are in different tanks which are not connected, it suffers low degradation and self discharge [15]. This fact makes them ideal for long-term energy storage. On the other hand, the lithium-ion batteries have higher efficiency, but are less scalable and suffer higher ageing degradation.

Therefore, the desired grid behaviour is that the RFB stores the extra energy from high-generation days to be used in the low-generation ones. In contrast, the Li-ion battery should store just the necessary daily energy to provide energy until the next solar panel generation cycle restarts. This procedure should be done smartly, minimizing the grid interaction and avoiding high grid power peaks that could lead to grid congestion.

## III. FORECAST

NNs operate by combining the information of the inputs through weights and activation functions. They are composed of a number of layers each of them containing a defined number of nodes, being the first layer of nodes the inputs and the last one the outputs. In a fully connected NN, to obtain each of the next layer nodes a weighted sum of the previous nodes is passed through an activation function. When the NN is trained using historical data, those weights are adjusted to its optimal values. The mathematical background of the training process is out of the scope of this work.

In this paper, fully connected NNs with a rectified linear unit (ReLU) activation function in all the nodes are used. Two different NNs are trained, one to predict PV generation and one for load. The prediction horizon for the MPC was selected as 24 hours due to the periodic behaviour of generation and load during a day. It has 30 minutes resolution, resulting in a forecast containing 48 values of electrical load and generation.

In order to decide the relevant inputs for each of the NNs, a Pearson correlation analysis was performed over all the inputs available resulting in a set of input candidates for each NN. Different temporal windows for historical data, input combination and NN structures were tested to select the proper ones.

The NN for PV generation forecast uses historical generation data and humidity values of the last 48 hours combined with the clear-sky irradiation forecast of the next 24 hours. The clear sky radiation consist in the ideal solar radiation in absence of clouds and is obtained using mathematical models. Its forecast is obtained using the simplified Solis model implemented in pvlib [16], which only requires the site location in coordinates. On the other hand, the NN for electrical consumption forecast is only provided with historical load values of the last 48 hours.

#### IV. MODEL PREDICTIVE CONTROLLER

The MPC controller uses a model of the considered grid and the generation and load forecasts to simulate future states of the system and calculate the optimal control actions over a prediction horizon. The online MPC solves the optimization problem at every time instant  $k$ , for a prediction horizon  $N$ , obtaining  $N$  control actions  $(u_{1|k}, u_{2|k}, u_{3|k}, \dots, u_{N-1|k})$  but applying only the first control action  $u_{1|k}$  [17]. Here, the notation  $u_{i|k}$  denotes the  $i$ -th value of the input vector along the prediction horizon given a time instant  $k$  along a simulation horizon. The aforementioned procedure is performed at every time instant using the measured system states to provide feedback.

##### A. Cost function

The MPC sets the control actions according to a user defined cost function. This cost function will be a sum of terms taking care of avoiding grid saturation, maximizing the self consumption and minimizing the batteries degradation. Quadratic cost functions will be used so the optimization problem can be solved efficiently [18].

##### 1) Batteries:

The batteries term has as objective to reduce batteries degradation. It consists in:

$$\begin{aligned} Q_{ESS} &= Q_{VFRB} + Q_{Li} \\ Q_{VFRB} &= \lambda_{pVFRB} \cdot p_{VFRB}^2 + \lambda_{socVFRB} \cdot SOC_{VFRB}^2 \\ Q_{Li} &= \lambda_{pLi} \cdot p_{Li}^2 + \lambda_{socLi} \cdot SOC_{Li}^2 \end{aligned} \quad (1)$$

where  $Q_i$  denotes the quadratic cost function and  $p_i$  the power demanded being  $i$  the subscript used to differentiate between a ESS, VFRB or lithium-ion battery. With respect to  $\lambda$  terms,  $\lambda_{pVFRB}$  and  $\lambda_{pLi}$  are weights that penalize the presence of high-power demands on the RFB and lithium-ion battery, respectively. Moreover,  $\lambda_{socVFRB}$  and  $\lambda_{socLi}$  reduce the ageing effect on batteries related to high SOC.

##### 2) Grid:

The grid term will have the double objective of maximizing self consumption and avoiding grid congestion. It consists in:

$$Q_{grid} = \lambda_{grid} \cdot p_{grid}^2, \quad (2)$$

where  $Q_{grid}$  is the grid quadratic cost function,  $p_{grid}$  is the grid power and the weight  $\lambda_{grid}$  is used to penalize the interaction with the grid, or in other words, to maximize the self consumption in the microgrid.

#### B. Models

##### 1) Grid Model:

The model of the grid used is based on the power balance equation. It consists in:

$$p_{pv} + p_{load} + p_{VFRB} + p_{Li} + p_{grid} = 0, \quad (3)$$

where  $p_{pv}$  is the solar panel generation,  $p_{load}$  is the load power demanded,  $p_{VFRB}$  is the VFRB power,  $p_{Li}$  is the Li-ion battery power and  $p_{grid}$  is the power exchanged with the grid.

##### 2) ESS Model:

Based on the Coulomb counting approach [19], the model provided to the MPC to predict the SOC evolution of both ESSs is the following:

$$SOC_{\beta}(k+1) = \begin{cases} SOC(k)_{\beta} - \frac{T_s \cdot \eta_{\beta}}{C_{\beta}} p_{\beta} & \text{if } p_{\beta} \leq 0, \\ SOC(k)_{\beta} - \frac{T_s}{C_{\beta} \cdot \eta_{\beta}} p_{\beta} & \text{if } p_{\beta} > 0, \end{cases} \quad (4)$$

where  $\beta = \{VFRB, Li\}$ ,  $k$  denotes the time instant,  $T_s$  is the sampling time and  $p_{\beta}$  is the power demanded to the battery, Besides,  $\eta_{\beta}$  is the ESS efficiency and  $C_{\beta}$  is the battery capacity. The efficiency  $\eta$  is considered to be a constant value for a certain battery, even if it really depends on the operation point. This assumption is adopted to avoid non linear formulation resulting from defining  $\eta_{\beta}$  as a  $f(p_b)$ .

#### C. Constraints

The MPC is a control method that can handle constraints so our system constraints were introduced into the MPC algorithm. The first constraint intends to avoid over-charging or deep discharges in batteries that could cause them degradation, i.e.,

$$SOC_{\beta}^{lo} < SOC_{\beta}(k) < SOC_{\beta}^{up} |_{\beta=\{VFRB, Li\}}, \quad (5)$$

where  $SOC_{\beta}^{lo}$  is the lower SOC limit of the ESS and  $SOC_{\beta}^{up}$  is the upper limit. These type of constraints are called hard constraints and one of their main issues is that they can lead to infeasible problems in the MPC-related optimization problem. Using soft constrains allows to cross the limits but paying a price in the cost function, adding reliability to the predictive

controller. Therefore, the previous constraint is substituted by the following soft constraint:

$$SOC_{\beta}^{lo} - \epsilon_{\beta}(k) < SOC_{\beta}(k) < \epsilon_{\beta}(k) + SOC_{\beta}^{up}, \quad (6)$$

where  $\beta = \{VRFB, Li\}$  and  $\epsilon_{\beta}$  is the SOC limit violation. The following term is added to the cost function (6) so the use of  $\epsilon_{\beta}$  is kept only for extreme cases:

$$Q_{soft} = \lambda_{soft,\beta} \cdot \epsilon_{\beta}(k)^2 |_{\beta=\{VRFB, Li\}}, \quad (7)$$

where  $\lambda_{soft,\beta}$  are the weights for the constrains violation. The higher they are, the more the MPC will try to avoid them.

Then, the power constraints of the batteries and grid must be added:

$$-p_{\alpha}^{max} \leq p_{\alpha}(k) \leq p_{\alpha}^{max}, \quad (8)$$

where  $\alpha = \{VRFB, Li, grid\}$ ,  $p_{\alpha}^{max}$  is the maximum power capabilities of the VRFB, Li-ion battery and grid (symmetrical bidirectional capabilities are assumed).

#### D. Mixed Logical Dynamic Model

The ESS model represented in (4) changes with the power flow sign so a modification is needed to use it in the optimization problem. Using a mixed logical dynamic (MLD) model, (4) is reformulated as:

$$\begin{aligned} SOC_{\beta}(k+1) &= SOC_{\beta}(k) + \\ &\frac{T_s}{C_{\beta}} \cdot \theta_{\beta}(k) \cdot p_{\beta}(k) \cdot \left(\eta_{\beta} - \frac{1}{\eta_{\beta}}\right) \\ &\quad - \frac{T_s \cdot \eta_{\beta}}{C_{\beta}} \cdot p_{\beta}(k) \\ p_{\beta}^{max} \cdot \theta_{\beta}(k) &\leq p_{\beta}(k) + p_{\beta}^{max} \\ -p_{\beta}^{max} \cdot \theta_{\beta}(k) &\leq -p_{\beta}(k) \end{aligned}$$

with  $\beta = \{VRFB, Li\}$ . The Boolean variable  $\theta_{\beta}$  is defined such that  $\theta_{\beta}(k) = 1 \leftrightarrow p_{\beta}(k) > 0$ .

Finally, an auxiliary variable is added  $y_{\beta}(k) = \theta_{\beta}(k) \cdot p_{\beta}(k)$  to avoid non-linear formulations, i.e.,

$$\begin{aligned} y_{\beta}(k) &\leq p_{\beta}^{max} \cdot \theta_{\beta}(k) \\ y_{\beta}(k) &\geq -p_{\beta}^{max} \cdot \theta_{\beta}(k) \\ y_{\beta}(k) &\leq p_{\beta}(k) + p_{\beta}^{max} \cdot (1 - \theta_{\beta}(k)) \\ y_{\beta}(k) &\geq p_{\beta}(k) - p_{\beta}^{max} \cdot (1 - \theta_{\beta}(k)). \end{aligned} \quad (9)$$

Then, (4) can be written as

$$\begin{aligned} SOC_{\beta}(k+1) &= SOC(k)_{\beta} + \frac{T_s}{C_{\beta}} \cdot y_{\beta}(k) \cdot \left(\eta_{\beta} - \frac{1}{\eta_{\beta}}\right) \\ &\quad - \frac{T_s \cdot \eta_{\beta}}{C_{\beta}} \cdot p_{\beta}(k). \end{aligned} \quad (10)$$

The MPC-related optimization problem can be formulated as:

$$\min \sum_{i=k}^{k+N-1} Q_{grid}(i) + Q_{ESS}(i) + Q_{soft}(i) \quad (11)$$

subject to

$$\begin{aligned} &Grid\ model\ (3), \\ &ESS\ model\ (10), \\ &Constraints\ (7)\ (8)\ (9) \end{aligned}$$

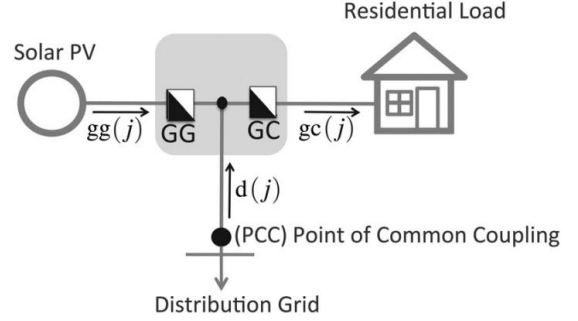


Fig. 3. Ausgrid households scheme [20]

## V. RESULTS

### A. Database

PV generation and load demand data used for the simulation were obtained from the Ausgrid dataset [20]. PV generation and load demand were recorded from 300 households in Australia for 3 years (July 2010 - July 2013) with the scheme shown in Fig. 3. Some households had also a controllable load represented by a hot water tank that was ignored considering that was probably adjusted to meet the PV generation. The closer households to the city of Newcastle that passed the clean methodology described in [20] were selected. From the 300 households, the households with the number {35, 73, 87, 88, 110, 119, 124, 144, 157, 176, 188, 201, 207, 256} were selected. Their solar PV generation and residential load were summed up to generate the complete microgrid generation and consumption.

Meteorological information of Newcastle area data were obtained from the National Solar Radiation Database (NSRDB), specifically from the Himawari based solar Resource data [21]. It provided historical meteorological information from the area of Newcastle with a temporal and space resolution of 60 minutes and 2 km between the years 2011 and 2015. Interpolation was performed to obtain a temporal resolution of 30 minutes.

### B. Forecast

Python and the Keras package were used to implement the NNs and the training optimizer was SGD. The programming environment used was Google Colab Pro version with the GPU hardware accelerator configuration. Clear sky forecast for the generation NN was obtained using the simplified Solis model implemented in pvlib [16]. In both NNs, 70% of the data was used for training, 15% for validation and 15% for testing.

The metrics used to evaluate the results were the mean squared error (MSE), the mean absolute error (MAE) and the weighted mean absolute error (WMAE) due to the regression

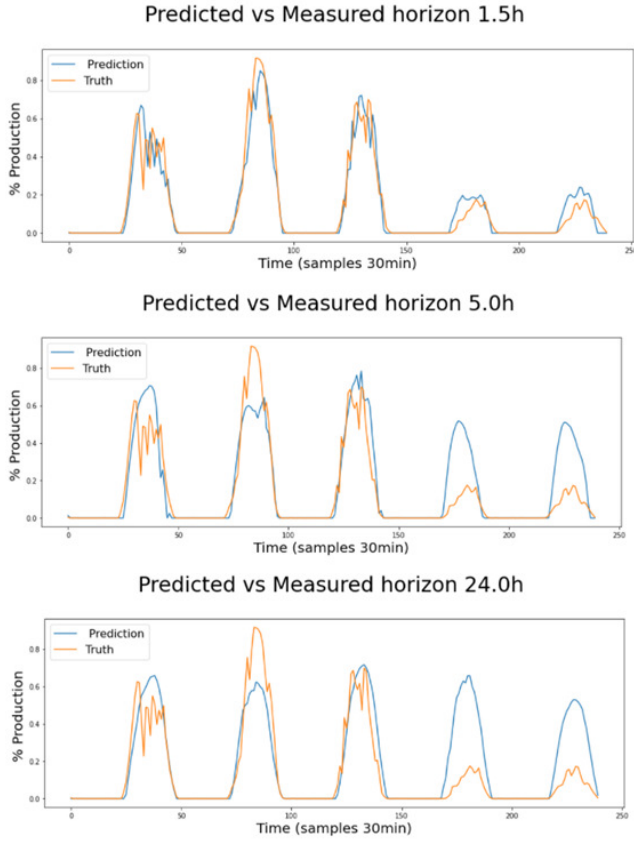


Fig. 4. PV forecast vs prediction horizon

nature of the stated problem. The metrics are defined by the following expressions:

$$MSE = \frac{\sum_{i=1}^N |P_{m,i} - P_{p,i}|^2}{N}, \quad (12)$$

$$MAE = \frac{1}{N} \sum_{i=1}^N |P_{m,i} - P_{p,i}|, \quad (13)$$

$$WMAE = \frac{\sum_{i=1}^N |P_{m,i} - P_{p,i}|}{\sum_{i=1}^N P_{m,i}}, \quad (14)$$

where  $P_{m,i}$  is the measured value and  $P_{p,i}$  is the predicted value at the instant  $i$  and  $N$  the total number of predictions or measurements. The units for the  $MSE$  and  $MAE$  are kWh, being the same ones of  $P$ . With respect to the  $WMAE$ , the units are dimensionless but can be presented in percentage multiplying per cent equation (14).

To avoid interference of the variables magnitude in the metrics evaluation, predictions and values are normalized before calculating the metrics. Different sets of inputs, temporal windows for historical data and NN structures were tested in order to obtain the optimal load and generator predictors.

For PV generation, the input candidates were the clear-sky irradiation and the environmental temperature, humidity, wind and generation historical values. The temporal window of historical data varied from 1 to 5 days. The NN structures tested the combination of a first hidden layer with values

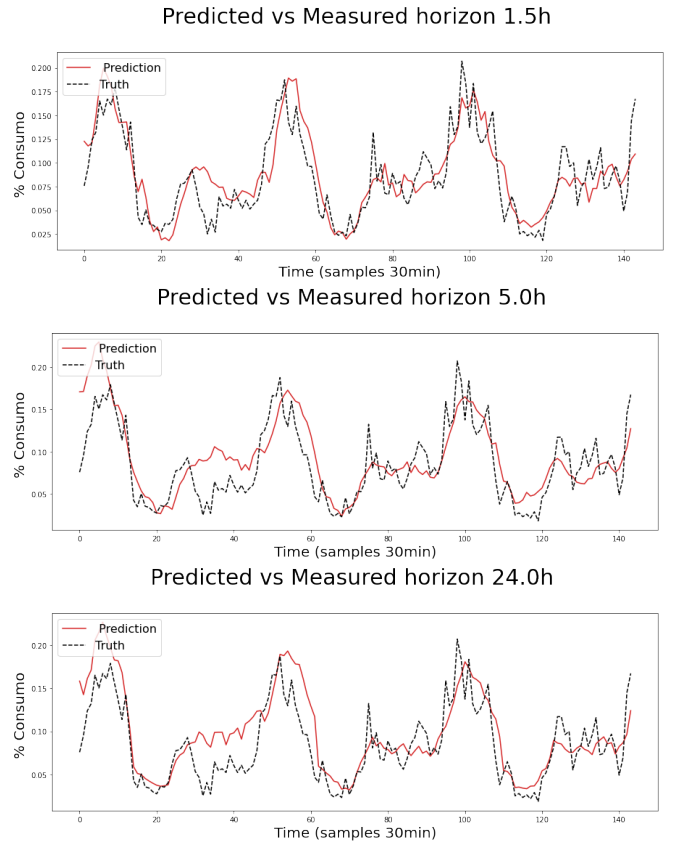


Fig. 5. Electrical consumption forecast vs prediction horizon

{512, 1024}, a second layer with values {64, 256} and a third layer with values {0, 64}.

The best results were obtained using historical generation data and humidity values of the last 48 hours and the clear-sky irradiation 24 hours forecast. The best NN structure consists in an input layer of 240 nodes, an output layer of 48 nodes and three hidden layers of 524, 64 and 64 nodes respectively. The following results were obtained:

- MSE: 0,00976
- MAE: 0,04839
- WMAE: 29,56 %

Fig. 4 includes the prediction and true values in sunny and cloudy days considering values predicted with different prediction horizons. When the prediction horizon is long, the NNs cannot predict much more than an average value influenced by the last days as it is not supplied with any weather forecast. However, whenever the prediction horizon is reduced, it adapts reaching much more accurate values. As expected, biggest errors appear in highly cloudy days.

For electrical consumption, the input candidate was just its historical values. The temporal window of historical data varied from 1 to 5 days. The NN structures tested there the same combination of three layers described previously for the PV production. The best results were obtained using historical values of the last 48 hours. The best NN structure consists in an input layer of 96 nodes, an output

layer of 48 nodes and three hidden layers of 1024, 256 and 64 nodes respectively. The following results were obtained:

- MSE: 0.00461
- MAE: 0.03795
- WMAE: 38,31 %

For load consumption, the MSE and MAE are lower meaning that the prediction error is lower in absolute value. However, analysing the WMAE, it is observed that the relative error is bigger, which is understandable considering that only historical data is supplied. Its performance is shown in Fig. 5, the NN is able to provide an approximate prediction even in long prediction horizons that is closely adjusted to reality when the prediction horizon is reduced.

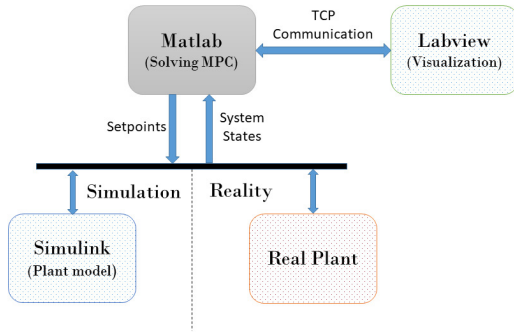


Fig. 6. Implementation Scheme

TABLE I  
SYSTEM PARAMETERS

Parameter	Value
$C_{VRFB}$	400kWh
$C_{Li}$	65kWh
$P_{VRFB}^{max}, P_{VRFB}^{min}$	+10 kW
$P_{Li}^{max}, P_{Li}^{min}$	+12 kW
$P_{grid}^{max}, P_{grid}^{min}$	+20 kW
$SOC_{VRFB}^{lo}, SOC_{Li}^{lo}$	0.1
$SOC_{VRFB}^{up}, SOC_{Li}^{up}$	0.9
$\lambda_{socVRFB}$	0.001
$\lambda_{socLi}$	30
$\lambda_{pVRFB}$	5
$\lambda_{pLi}$	2
$\lambda_{grid}$	50
$\lambda_{soft}$	$10^7$

### C. Model predictive controller design

The MPC was implemented in Matlab (version 2021b) using YALMIP as parser and the Gurobi solver [22]. For simulation purposes, the grid model is implemented in Simulink using its generic Li-ion battery model [23], while (10) was used to model the VRFB. LabVIEW2021 is used for data acquisition

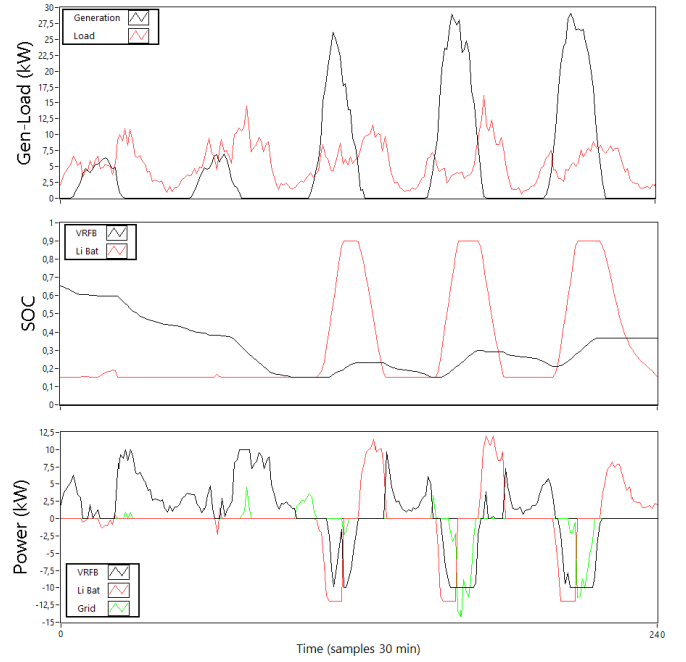


Fig. 7. MSC simulation

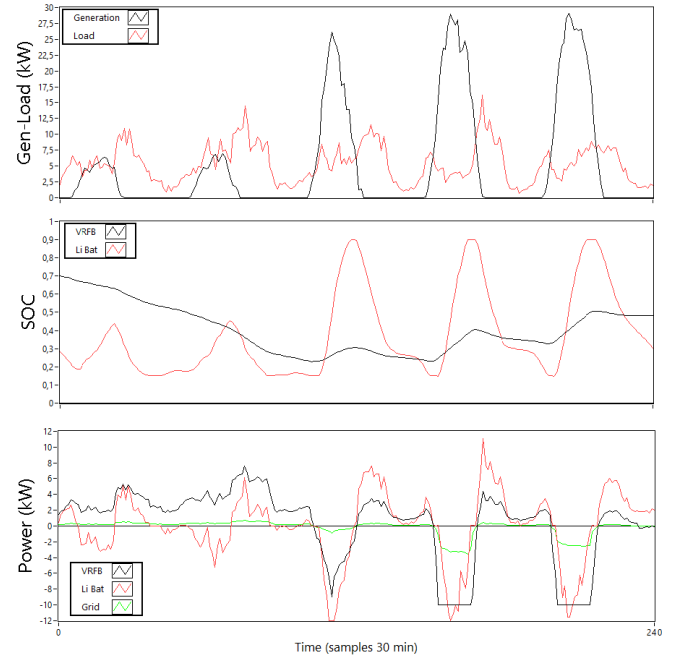


Fig. 8. Ideal MPC simulation

and visualization. The data sampling time is 30 minutes, the system states measured are sent to Matlab which solves the MPC-related optimization problem for the established prediction horizon of 24 hours. In the simulation case, the next 30 minutes are simulated in Simulink and system states are acquired from it, while in the real case they would be measured from the real plant (the real system is not available). Finally, data are sent from Matlab to Labview using TCP communication protocol (Fig. 6). The characteristics of the different components of the grid are shown in Table I.

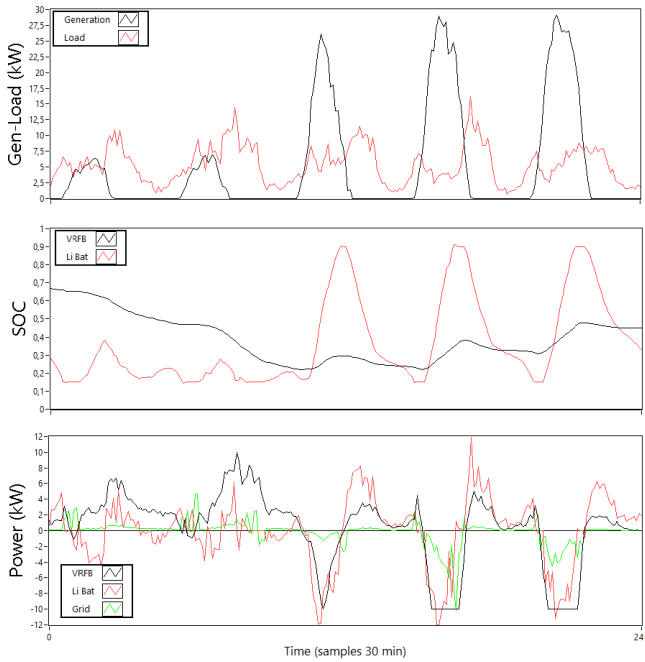


Fig. 9. Real MPC simulation

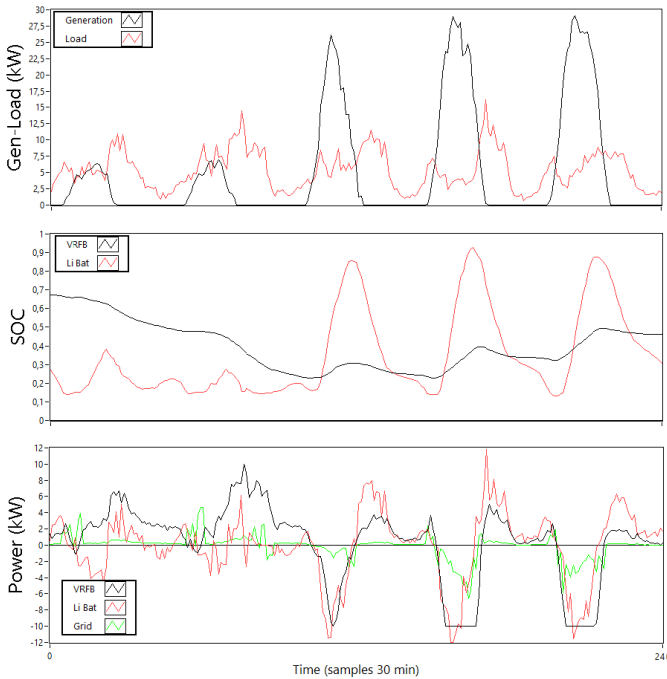


Fig. 10. Real MPC with softer constrains simulation

The desired grid behaviour was described in Section II and, through different simulations, the optimal weights were selected. Hence,  $\lambda_{socVRFB}$  is extremely low in order to allow the VRFB to store energy considering horizons higher than 24 hours (it has to store energy from sunny days to use it in cloudy days). In contrast,  $\lambda_{socLi}$  is higher to ensure that the Li-ion battery does not store more energy than the one necessary until the next day, which would increase its degradation and reduce its storage capabilities in the next day.

In order to maximize self consumption and avoid grid

saturation,  $\lambda_{grid}$  is the highest of all power weights. This fact ensures that the microgrid will preferably use other power sources to balance its generation and consumption and will avoid high power peaks with the grid. Besides,  $\lambda_{pVRFB}$  is higher than  $\lambda_{pLi}$  as the Li-ion battery should be in charge of the 24 hours energy loop while the VRFB should mainly compensate the 24 hours energy imbalance. Finally,  $\lambda_{soft}$  is kept sufficiently high to avoid constraint violations.

Initially, the performance of the classic method of maximizing self consumption (MSC) is analysed. Any generation and load difference is compensated by the Li-ion battery if it is between its power and SOC limits. The part that cannot be handle by the Li-ion battery is handled by the VRFB if it is within its power and SOC limits. The rest of power is managed by the grid.

The MSC performance is shown in Fig. 7. Future consumption and generation are not considered, leading to early charges in the day and early discharges at night of the Li-ion battery. When the Li-ion battery is not available during the generation peak, a large power has to be fed to the grid which could cause grid saturation. The Li-ion battery remains at high SOC's unnecessary increasing its degradation. At nights, it is especially noticeable that the Li-ion battery and VRFB are not combined properly, as the first one provides all the energy until it reaches its SOC limits and the VRFB has then to provide all the energy. This results in higher peak currents in both compared to partially using both all night.

Now, the ideal performance of the MPC is discussed, real future values of generation and consumption are provided to the MPC. An example of its performance is shown in Fig. 8. The Li-ion battery is not kept at high SOC's unnecessary and the VRFB is used to support it reducing the peak currents. During highly cloudy days, the MPC uses the VRFB to provide most of the energy avoiding high currents on it by using the Li-ion battery previously charged when the load was low.

During high generation days, the MPC takes into consideration the high generation prediction and avoids an early charge of the Li-ion battery. It is kept available to absorb the power peak that otherwise it would have to be fed to the grid (grid congestion issues). To do so the MPC maximizes the use of the VRFB due to its high capacity and manages the interaction with the grid so the maximum power fed is kept as low as possible. For all this reason it is considered that the ideal MPC highly overcomes MSC performance.

Now prediction errors are considered, the NNs forecast values for generation and consumption are provided to the MPC. Therefore, the difference between the energy imbalance predicted and the real energy imbalance has to be managed. It is set to be absorbed by the Li-ion battery whenever it is within its SOC soft limits and its power limits. The part of the prediction error that cannot be handled by the Li-ion battery will be handled by the grid. In Fig. 9, we can observe how the performance is modified when we incorporate the prediction errors to the MPC. As before, the Li-ion battery and the VRFB work together to avoid high peak currents in each of them. The

main issue found is the appearance of higher power peaks with the grid. The Li-ion battery reaches its SOC limit as the prediction was not perfect and it handles the prediction errors. This also causes the Li-ion battery to stay longer time at high SOC levels unnecessarily.

In order to reduce the grid power peaks previously mentioned, we can allow the Li-ion battery to use part of the SOC gap reserved for the soft constraints. By reducing  $SOC_{Li}^{lo}$  to 0.85 and decreasing its  $\lambda_{soft}$  to  $10^5$  we provide the Li-ion battery with some margin to exceed the SOC limits to avoid high grid power peaks. The results are shown in Fig. 10, in which we can observe how the grid power peaks and the flat high SOC regions of the Li-ion battery are reduced. It is important to mention that the correct balance has to be found, as making the constraints too soft could cause overcharges or deep discharges in the battery and feasibility issues in the MPC. It is concluded that the real MPC performance still overcomes the performance of the MSC, reducing most of the problems mentioned in the MSC performance.

## VI. CONCLUSIONS

In this work, an online predictive controller has been implemented to manage a microgrid with PV generation, electrical consumption, a Li-ion battery, a vanadium redox flow battery (VRFB) and connection to the grid. A predictive controller was feed with generation and load forecasts provided by two different NNs. Real data from Australian households have been used. The model predictive control (MPC) strategy used in this paper has been shown useful to deal the with the problems derived from using the classical method of maximizing self consumption (MSC). MPC can avoid early of the energy storage system (ESS) charges during high generation days, keeping the ESS available for the generation power peak and avoiding high power peaks with the grid that could cause grid congestion. The MPC also takes into consideration the ESS degradation reducing their peak currents and avoids remaining at high state of charge (SOC) levels when it is not necessary.

As expected, the better the generation and load forecast are, the better is the MPC performance. The best performance has been obtained when real future values are provided to the MPC, however, it has been shown that the real MPC with neural networks (NNs) forecast can also solve most of the MSC problems if it is set correctly. Improving the forecast accuracy by using future weather forecast or implementing methods to deal with the uncertainty could be possible future step to continue improving the MPC performance.

## REFERENCES

- [1] H. Schermeyer, M. Studer, M. Ruppert, and W. Fichtner, "Understanding distribution grid congestion caused by electricity generation from renewables," *IFIP Advances in Information and Communication Technology*, DOI 10.1007/978-3-319-66553-5\_6, pp. 78–89, 2017.
- [2] G. de Oliveira e Silva and P. Hendrick, "Photovoltaic self-sufficiency of belgian households using lithium-ion batteries, and its impact on the grid," *Applied Energy*, vol. 195, DOI 10.1016/j.apenergy.2017.03.112, pp. 786–799, 2017.
- [3] L. Yanxue, W. Gao, and Y. Ruan, "Performance investigation of grid-connected residential PV-battery system focusing on enhancing self-consumption and peak shaving in Kyushu Japan," *Renewable Energy*, vol. 127, DOI 10.1016/j.renene.2018.04.074, 2018.
- [4] U. R. Nair and R. Costa-Castelló, "A model predictive control-based energy management scheme for hybrid storage system in islanded microgrids," *IEEE Access*, vol. 8, DOI 10.1109/ACCESS.2020.2996434, pp. 97 809–97 822, 2020.
- [5] A. Cecilia, M. Serra, and R. Costa-Castelló, "Nonlinear adaptive observation of the liquid water saturation in polymer electrolyte membrane fuel cells," *Journal of Power Sources*, vol. 492, DOI 10.1016/j.jpowsour.2021.229641, p. 229641, 2021.
- [6] J. L. Anderson, J. J. Moré, P. F. Puleston, V. Roda, and R. Costa-Castelló, "Control super-twisting con adaptación basada en cruce por cero. Análisis de estabilidad y validación," *Revista Iberoamericana de Automática e Informática industrial*, vol. 20, DOI 10.4995/riai.2022.17214, no. 1, p. 104–114, 2022.
- [7] A. Clemente and R. Costa-Castelló, "Redox flow batteries: A literature review oriented to automatic control," *Energies*, vol. 13, DOI 10.3390/en13174514, p. 4514, 2020.
- [8] A. Barré, B. Deguilhem, S. Grolleau, M. Gerard, F. Suard, and D. Riu, "A review on lithium-ion battery ageing mechanisms and estimations for automotive applications," *Journal of Power Sources*, vol. 241, DOI 10.1016/j.jpowsour.2013.05.040, p. 680–689, 2013.
- [9] D. Stroe, M. Swierczynski, A. Stan, and R. Teodorescu, "Accelerated lifetime testing methodology for lifetime estimation of lithium-ion batteries used in augmented wind power plants," *IEEE Transactions on Industry Applications*, vol. 50, DOI 10.1109/IECC.2013.6646769, pp. 690–698, 2013.
- [10] U. R. Nair, M. Sandelic, A. Sangwongwanich, T. Dragicevic, R. Costa-Castelló, and F. Blaabjerg, "Grid congestion mitigation and battery degradation minimisation using model predictive control in PV-based microgrid," *IEEE Transactions on Energy Conversion*, DOI 10.1109/TEC.2020.3032534, pp. 1–11, 2021. [Online]. Available: <https://doi.org/10.1109/TEC.2020.3032534>
- [11] M. A. Bermeo-Ayerbe, C. Ocampo-Martinez, and J. Diaz-Rozo, "Data-driven energy prediction modeling for both energy efficiency and maintenance in smart manufacturing systems," *Energy*, vol. 238, DOI <https://doi.org/10.1016/j.energy.2021.121691>, p. 121691, 2022.
- [12] E. Ratnam, S. Weller, C. Kellett, and A. Murray, "Residential load and rooftop PV generation: An australian distribution network dataset," *International Journal of Sustainable Energy*, DOI 10.1080/14786451.2015.1100196, 2015.
- [13] M. Abdel-Nasser and K. Mahmoud, "Accurate photovoltaic power forecasting models using deep LSTM-RNN," *Neural Computing and Applications*, vol. 31, DOI 10.1007/s00521-017-3225-z, 2019.
- [14] H. Shi, M. Xu, and R. li, "Deep learning for household load forecasting – a novel pooling deep rnn," *IEEE Transactions on Smart Grid*, vol. PP, DOI 10.1109/TSG.2017.2686012, pp. 1–1, 2017.
- [15] T. Puleston, A. Clemente, R. Costa-Castelló, and M. Serra, "Modelling and estimation of vanadium redox flow batteries: A review," *Batteries*, vol. 8, DOI 10.3390/batteries8090121, p. 121, 2022.
- [16] V. Kallio and A. Riihelä, "Comparative validation of clear sky irradiance models over Finland," in *IGARSS 2018 - 2018 IEEE International Geoscience and Remote Sensing Symposium*, DOI 10.1109/IGARSS.2018.8519270, pp. 1199–1202, 2018.
- [17] U. Raveendran Nair, M. Sandelic, A. Sangwongwanich, T. Dragicevic, R. Costa-Castelló, and F. Blaabjerg, "An analysis of multi objective energy scheduling in PV-bess system under prediction uncertainty," *IEEE Transactions on Energy Conversion*, vol. PP, DOI 10.1109/TEC.2021.3055453, 2021.
- [18] H.-J. Lüthi, "Convex optimization: Stephen Boyd and Lieven Vandenberghe," *Journal of the American Statistical Association*, vol. 100, DOI 10.2307/27590646, pp. 1097–1097, 2005.
- [19] K. Ng, C.-S. Moo, Y.-P. Chen, and Y.-C. Hsieh, "Enhanced Coulomb counting method for estimating state-of-charge and state-of-health of lithium-ion batteries," *Applied Energy*, vol. 86, DOI 10.1016/j.apenergy.2008.11.021, pp. 1506–1511, 2009.
- [20] E. Ratnam, S. Weller, C. Kellett, and A. Murray, "Residential load and rooftop PV generation: An australian distribution network dataset," *International Journal of Sustainable Energy*, DOI 10.1080/14786451.2015.1100196, 2015.
- [21] NREL. Nsrdb: National solar radiation database. [Online]. Available: <http://https://nslrdb.nrel.gov/>
- [22] Gurobi, "Gurobi optimizer reference manual," 2022. [Online]. Available: <https://www.gurobi.com>
- [23] MathWorks. Generic battery model. [Online]. Available: <https://es.mathworks.com/help/physmod/sps/powersys/ref/battery.html>